

Output Impedance Diffusion into Lossy Power Lines

Pooya Monshizadeh, Nima Monshizadeh, Claudio De Persis, and Arjan van der Schaft

Abstract—Coping with lossy distribution lines has been an obstacle in control and stability of power networks. Often, imposing an inductive output impedance to the sources has been considered as a means to justify the commonly adopted assumption of purely inductive lines, which in turn facilitates the construction of energy-based Lyapunov functions. In this paper, we propose a measure to evaluate the inductivity of the resulting grid, and investigate the extent to which the output impedance can affect the behavior of the distribution lines seen from the voltage source outputs. We show analytically that the more connected the network is, the more the output impedance diffuses into the network.

Index Terms—Power network, Output impedance, Graph theoretical models, Laplacian matrix, Kron reduction

I. INTRODUCTION

A microgrid is a small power network consisting of distributed sources and loads which can be seen as one entity from the large area electrical grid. In the case of a fault occurring in the main network, such an entity can become isolated and go to the so-called *islanded mode*. In this situation, since few loads and sources are involved, the power consumption and generation becomes highly erratic. To control such a system in terms of voltage control and frequency stabilization, many methods have been proposed during the last few decades. Among these, *droop controllers* have been the main and highly-accepted solution, however there are still on-going researches and debates over this method in order to improve its performance and overcome its limitations [1]. In view of the stability analysis and performance of these controllers, coping with lossy lines is perhaps the most challenging problem [2]–[6]. While energy-based Lyapunov functions can be constructed in the lossless case, such construction is far from trivial when power line losses are taken into account [7]–[12].

In some articles, the inductive output filter (or the transformer output) is assumed to dominate the resistive behavior of the lines [7]. If the inductance size is not large enough,

Pooya Monshizadeh and Arjan van der Schaft are with the Johann Bernoulli Institute for Mathematics and Computer Science, University of Groningen, 9700 AK, the Netherlands, p.monshizadeh@rug.nl, a.j.van.der.schaft@rug.nl

Nima Monshizadeh is with the electrical engineering division, University of Cambridge, CB3 0FA, United Kingdom, n.monshizadeh@eng.cam.ac.uk

Claudio De Persis is with the Electronics, Power and Energy Conversion Group, University of Groningen, 9747 AG, the Netherlands, c.de.persis@rug.nl

This work is supported by the STW Perspectief program "Robust Design of Cyber-physical Systems" under the auspices of the project "Energy Autonomous Smart Microgrids".

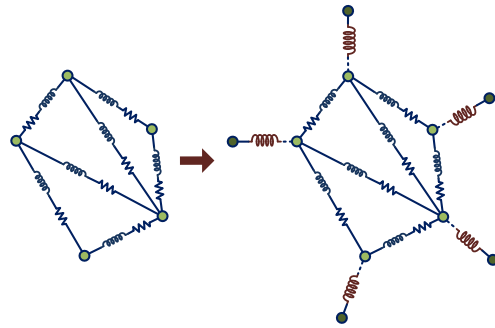


Fig. 1. Inductive outputs are typically added to the sources in order to assume inductive lines for the resulting network.

a natural way to bypass the aforementioned obstacle is to put a large inductor in the output port of the sources (see Figure 1). However, due to the inductor size, cost, and the unavoidable increase in the DC-side voltage, the method has been considered inefficient [2], [13]. As an alternative, the concept of *virtual output impedance* was used to decouple active and reactive power flow [14], and to justify the lossless lines assumption [15], [16]. In case of a virtual inductor, an emulation of a realistic inductor is carried out by decreasing the desired output voltage, proportional to the time derivative of the measured current. Since the distribution lines in low voltage microgrids are mainly resistive [17], in an analogous method, resistive outputs are attached to the sources to make the lines dominantly resistive. In that case, *inverse droop control* is employed where frequency is regulated via the reactive power, and the voltages through the active power [18].

Besides the aforementioned motive, the virtual output impedance is also employed to correct the reactive power sharing error due to the line mismatch [3], [19], [20], supply harmonics to nonlinear loads [21], [2], [22], share current among sources resilient to parameters mismatch and synchronization error [23], decrease sensitivity to line impedance unbalances [4], [24], reduce the circulating currents [25], limit output current during voltage sags [26], minimize circulating power [27], and damp the *LC* resonance in the output filter [14]. Although an inductive output impedance, either resulting from the inherent output filter or the added output impedance, is widely considered as a tool to enforce an inductive behavior for the resulting network, no theoretical analysis has been carried out to verify the feasibility or quantify the effectivity of this method. Note that the output impedance cannot be chosen arbitrary large, since a large impedance substantially boosts the voltage sensitivity to current fluctuations, and results in high frequency noise amplification [14].

A reasonable approach to quantify the inductivity of the overall network, is to look at the edges of the reduced graph obtained from eliminating the internal nodes (the light green nodes in Figure 1). However, this requires that an electrical network can be built such that its mathematical description matches that of the reduced model. While this is always possible in purely resistive networks [28], such synthesis is generally not feasible in an RL network [29]. An exception to this, is the network where the distribution lines are assumed to be made of the same material and hence share the same inductivity to resistivity ratio. The lines with such a property are referred to as *homogeneous* lines. In that case, the resulting reduced model can be realized again with homogeneous RL links [30], [31]. However in our setup, as the output impedances have different inductivity to resistivity ratio compared to the homogeneous lines, the overall network is not homogeneous anymore. Hence, a different and novel treatment is required to evaluate the inductivity behavior of the overall network.

In this paper, we examine the effect of the output impedances on a homogeneous distribution system by proposing a quantitative measure for the inductiveness of the resulting heterogeneous network. Similarly, a dual measure is defined for the case of resistive output in dominantly resistive networks. We identify bounds on the diffusion of output impedances into the grid lines. One can design the required output impedance to guarantee a desired behavior, using only the *algebraic connectivity* of the graph.

In Section II the method and the definitions are provided and the proposed measure is analytically driven for different cases of output inductors and resistors. Later in Section III, methods for choosing the optimum values of output impedance are investigated, such that their effect on the network inductivity measure is maximized. Finally, in Section IV the proposed measure is evaluated with the Kron reduction in phasor domain.

II. METHOD

Consider a homogeneous electrical network with an arbitrary topology, where we assume that all the sources and loads are connected to the grid via power converter devices (inverters) [32]. The network of this grid is represented by a connected and weighted undirected graph $\mathcal{G}(\mathcal{V}, \mathcal{E}, \Gamma)$. The nodes $\mathcal{V} = \{1, \dots, n\}$ represent the inverters, and the edge set \mathcal{E} accounts for the distribution lines. The total number of edges is denoted by m , i.e., $|\mathcal{E}| = m$. The edge weights are collected in the diagonal matrix Γ , and will be specified later.

For an undirected graph \mathcal{G} , the incidence matrix B is obtained by assigning an arbitrary orientation to the edges of \mathcal{G} and defining

$$b_{ik} = \begin{cases} +1 & \text{if } i \text{ is the tail of arc } k \\ -1 & \text{if } i \text{ is the head of arc } k \\ 0 & \text{otherwise} \end{cases}$$

with b_{ik} being the (i, k) th element of B .

We start our analysis with the voltages across the edges of the graph \mathcal{G} . Let $R_e \in \mathbb{R}^{m \times m}$ and $L_e \in \mathbb{R}^{m \times m}$ be the

diagonal matrices of resistance and inductance of edges. We have

$$R_e I_e + L_e \dot{I}_e = B^T V, \quad (1)$$

where $I_e \in \mathbb{R}^m$ denotes the current of edges with the same orientation of the incidence matrix, and $V \in \mathbb{R}^n$ represents the voltages at the nodes. Let $r \in \mathbb{R}$ and $l \in \mathbb{R}$ denote the resistance and inductance per length unit, respectively. In addition, let the weight matrix Γ be specified as

$$\Gamma = \text{diag}(\gamma) := \text{diag}(\tau_1^{-1}, \tau_2^{-1}, \dots, \tau_m^{-1}) \quad (2)$$

with τ_k denoting the actual distance between nodes i and j , for each $k \sim \{i, j\}$. Since the network is assumed to be homogeneous, we can rewrite (1) as [31]

$$r I_e + l \dot{I}_e = \Gamma B^T V,$$

Hence, $r B I_e + l B \dot{I}_e = B \Gamma B^T V$, and

$$r I + l \dot{I} = \mathcal{L} V, \quad (3)$$

where $I := B I_e$ is the vector of nodal current injections. The matrix $\mathcal{L} = B \Gamma B^T$ is the Laplacian matrix of the graph $\mathcal{G}(\mathcal{V}, \mathcal{E}, \Gamma)$ with the weight matrix Γ .

As mentioned before, once output impedances are added to the network, the network is not homogeneous anymore. Consequently, the overall model can not be described by (3). To tackle this problem, we depart from the simplified equation (3) and consider the more general case in which the network is described by

$$R I + L \dot{I} = \mathcal{L} V, \quad (4)$$

where $R \in \mathbb{R}^{n \times n}$ and $L \in \mathbb{R}^{n \times n}$ are matrices associated closely with the resistances and inductances of the lines, respectively. Note that this description cannot necessarily be realized with passive RL elements. Therefore, while the inductivity behavior of the homogeneous network (3) is simply determined by the ratio $\frac{l}{r}$, the one of (4) cannot be trivially quantified.

The idea here is to promote the rate of convergence as a suitable metric quantifying the inductivity/resistivity of the network. For the network dynamics in (3), the rate of convergence of the solutions is determined by the ratio $\frac{r}{l}$. The more inductive the lines are, the slower the rate of convergence is. Now, we seek for a similar property in (4). Notice that the solutions of (3) are damped with corresponding eigenvalues of $L^{-1}R$. Throughout the paper, we assume that all eigenvalues of the matrix $L^{-1}R$ are positive and real. It will be shown that this assumption is satisfied for all the various cases considered in this paper. Figure 2 sketches the behavior of homogeneous solutions of (4). Among all the solutions, we choose the fastest one as our measure for inductivity, and the slowest one for resistivity of the network. Opting for these worst case scenarios allows us to guarantee a prescribed inductivity or resistivity ratio by proper design of output impedances. These choices are formalized in the following definitions.

Definition 1 Let $I(t, I_0)$ be the homogeneous solution of (4) with initial condition $I_0 \in \text{im } B$. Let the set $M_L \subseteq \mathbb{R}^+$ be given by

$$M_L := \{\sigma \in \mathbb{R}^+ \mid \exists \mu \text{ s.t.} \\ \|I(t, I_0)\| \geq \mu e^{-\sigma t} \|I_0\|, \forall t \in \mathbb{R}^+, \forall I_0 \in \text{im } B\}.$$

Then we define the *Network Inductivity Ratio* (NIR) as

$$\Psi_{\text{NIR}} := \frac{1}{\inf(M_L)}.$$

□

Definition 2 Let $I(t, I_0)$ be the homogeneous solution of (4) with initial condition $I_0 \in \text{im } B$. Let the set $M_R \subseteq \mathbb{R}^+$ be given by

$$M_R := \{\sigma \in \mathbb{R}^+ \mid \exists \mu \text{ s.t.} \\ \|I(t, I_0)\| \leq \mu e^{-\sigma t} \|I_0\|, \forall t \in \mathbb{R}^+, \forall I_0 \in \text{im } B\}.$$

We define the *Network Resistivity Ratio* (NRR) as

$$\Psi_{\text{NRR}} := \sup(M_R).$$

□

Note that the set M_L is bounded from below and M_R is bounded from above by definition. Interestingly, in case of the homogeneous network (3), i.e. without output impedances, we have $\Psi_{\text{NIR}} = \frac{\ell}{r}$ and $\Psi_{\text{NRR}} = \frac{r}{\ell}$, which are intuitive measures to reflect the inductivity and resistivity of the homogeneous network (3).

A. Inductive Output Impedance

Consider the output inductances appended to the network. Note that the injected currents pass through the output impedances, as shown in Figure 3. Therefore

$$V = V_o - \ell_o \dot{I}, \quad (5)$$

where $\ell_o \in \mathbb{R}^+$ is the (uniform) output inductance added to all the nodes, and $V_o \in \mathbb{R}^n$ is the voltage of the augmented nodes (the dark green nodes in Figure 1). Recall that the injected currents satisfy the equation (3). Having (3) and (5) we obtain

$$rI + (\ell_o \mathcal{L} + \ell \mathcal{I}) \dot{I} = \mathcal{L} V_o, \quad (6)$$

where $\mathcal{I} \in \mathbb{R}^{n \times n}$ denotes the identity matrix, and \mathcal{L} is the Laplacian matrix of \mathcal{G} as before. Note that in view of equation (4), the matrices R and L are given by $R = r\mathcal{I}$ and $L = \ell_o \mathcal{L} + \ell \mathcal{I}$ in this case. The eigenvalues of the product $L^{-1}R$ are all positive and real, and are given by $\lambda_i(L^{-1}R) = r\lambda_i^{-1}(\ell_o \mathcal{L} + \ell \mathcal{I})$. To calculate the measure Ψ_{NIR} for the inductivity of the resulting network, we investigate the rate of convergence of the homogeneous solution of (6). This brings us to the following theorem:

Theorem 1 Consider a homogeneous distribution network with the resistance per length unit r , inductance per length unit ℓ , and output inductors ℓ_o . Then the network inductivity ratio is given by

$$\Psi_{\text{NIR}} = \frac{\ell_o \lambda_2 + \ell}{r},$$

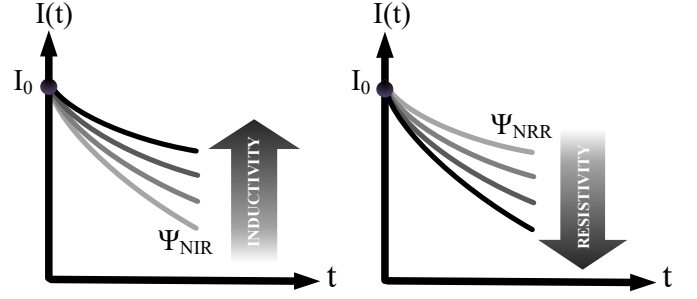


Fig. 2. Worst cases are selected for inductivity and resistivity measures.

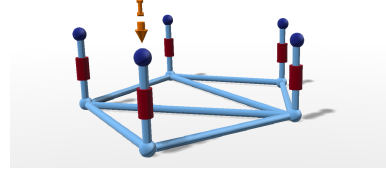


Fig. 3. The injected currents at the nodes of the original graph pass through the added output impedance.

where λ_2 is the algebraic connectivity of the graph $\mathcal{G}(\mathcal{V}, \mathcal{E}, \Gamma)$.

Proof: The homogeneous solution to (6) is $I(t) = e^{-r(\ell_o \mathcal{L} + \ell \mathcal{I})^{-1}t} I_0$. Note that \mathcal{L} is positive semidefinite and thus the matrix $\ell_o \mathcal{L} + \ell \mathcal{I}$ is invertible. By the spectral decomposition $\mathcal{L} = \mathcal{U} \Lambda \mathcal{U}^T$, we find that

$$I(t) = e^{-r(\mathcal{U}(\ell_o \Lambda + \ell \mathcal{I})\mathcal{U}^T)^{-1}t} I_0 = \mathcal{U} e^{-r(\ell_o \Lambda + \ell \mathcal{I})^{-1}t} \mathcal{U}^T I_0 \\ = \left[\frac{1}{\sqrt{n}} \mathbf{1} \quad \tilde{\mathcal{U}} \right] e^{-r \begin{bmatrix} \frac{1}{\ell} & 0 \\ 0_{(n-1) \times 1} & \tilde{\Lambda}^{-1} \end{bmatrix} t} \begin{bmatrix} \frac{1}{\sqrt{n}} \mathbf{1}^T \\ \tilde{\mathcal{U}}^T \end{bmatrix} I_0,$$

where $\tilde{\Lambda} = \text{diag } \tilde{\lambda} = \text{diag}\{\ell_o \lambda_2 + \ell, \dots, \ell_o \lambda_n + \ell\}$ and $0 < \lambda_2 < \lambda_3 < \dots < \lambda_n$ are nonzero eigenvalues of \mathcal{L} . Noting that by the Kirchhoff Law, $\mathbf{1}^T I_0 = 0$, we have

$$I(t) = \tilde{\mathcal{U}} e^{-r\tilde{\Lambda}^{-1}t} \tilde{\mathcal{U}}^T I_0 = \left(\sum_{i=1}^{n-1} e^{-r\tilde{\lambda}_i^{-1}t} \tilde{\mathcal{U}}_i \tilde{\mathcal{U}}_i^T \right) \left(\sum_{i=1}^{n-1} \alpha_i \tilde{\mathcal{U}}_i \right) \\ = \sum_{i=1}^{n-1} \alpha_i e^{-r\tilde{\lambda}_i^{-1}t} \tilde{\mathcal{U}}_i,$$

where $\tilde{\mathcal{U}}_i$ denotes the i th column of $\tilde{\mathcal{U}}$, and we used again $\mathbf{1}^T I_0 = 0$ to write I_0 as the linear combination $I_0 = \sum_{i=1}^{n-1} \alpha_i \tilde{\mathcal{U}}_i$. Hence

$$\|I(t)\|^2 = \sum_{i=1}^{n-1} \alpha_i^2 e^{-2r\tilde{\lambda}_i^{-1}t}. \quad (7)$$

Bearing in mind that $\|I_0\|^2 = \sum_{i=1}^{n-1} \alpha_i^2$, we conclude that

$$\|I(t)\| \geq e^{-\frac{r}{\ell_o \lambda_2 + \ell} t} \|I_0\|, \quad (8)$$

which yields $\Psi_{\text{NIR}} = \frac{\ell_o \lambda_2 + \ell}{r}$. Note that (8) holds with equality in case I_0 belongs to the span of the corresponding eigenvector of the second smallest eigenvalue of the Laplacian matrix \mathcal{L} . This completes the proof. ■

Theorem 1 provides a useful and easy-to-use measure that can be used to appropriately choose the output impedances in order to impose a desired degree of inductivity on the network. The only information required is the line parameters r , and ℓ , and the algebraic connectivity of the network; see [33] and [34] for more information of algebraic connectivity and its lower and upper bounds in various graphs.

Remark 1 Theorem 1 reveals the fact that: “The more connected the network is, the more the output impedance diffuses into the network.” \square

Remark 2 Note that (7) reveals also the existence of an upper bound on $\|I(t)\|$, namely

$$\|I(t)\| \leq e^{-\frac{r}{\ell_o \lambda_{\max} + \ell} t} \|I_0\|. \quad (9)$$

Hence the quantity $r^{-1}(\ell_o \lambda_{\max} + \ell)$, with λ_{\max} denoting the largest eigenvalue of the Laplacian matrix of \mathcal{G} , indicates the smallest rate of convergence, and is associated with the slowest solution of (6) (see Figure 2). \square

B. Resistive Output Impedance

Consider the output resistors r_o added to the network described by (3). We can model the resulting system as

$$rI + \ell \dot{I} = \mathcal{L}V, \quad V = V_o - r_o I.$$

The overall network can be described as

$$(r_o \mathcal{L} + r \mathcal{I})I + \ell \dot{I} = \mathcal{L}V_o. \quad (10)$$

Compared to the equation (4), here $R = r_o \mathcal{L} + r \mathcal{I}$ and $L = \ell \mathcal{I}$. Hence, similar to the inductive case, the matrix $L^{-1}R$ has positive real eigenvalues, and the network resistivity ratio in this case is obtained as follows:

Theorem 2 Consider a homogeneous distribution network with the resistance per length unit r , inductance per length unit ℓ , and output inductors ℓ_o . Then the network resistivity ratio is given by

$$\Psi_{\text{NRR}} = \frac{r_o \lambda_2 + r}{\ell},$$

where λ_2 is the algebraic connectivity of the graph $\mathcal{G}(\mathcal{V}, \mathcal{E}, \Gamma)$.

Proof: The proof can be constructed in an analogous way to the proof of Theorem 1 and is therefore omitted. \blacksquare

C. Inductive-Resistive Output Impedance

In most cases of practical interest, the output impedance consists of both inductive and resistive elements. In this section, we investigate the effect of the addition of such output impedances on the network inductivity ratio. The changes in network resistivity ratio can be studied similarly, and thus omitted here.

Consider the output impedances with the inductive part ℓ_o and the resistive component r_o (in series), added to the network (3). The overall network can be described as

$$rI + \ell \dot{I} = \mathcal{L}V, \quad V = V_o - r_o I - \ell_o \dot{I}.$$

Hence

$$(r_o \mathcal{L} + r \mathcal{I})I + (\ell_o \mathcal{L} + \ell \mathcal{I})\dot{I} = \mathcal{L}V_o. \quad (11)$$

In view of equation (4), the matrices R and L are given by $R = r_o \mathcal{L} + r \mathcal{I}$ and $L = \ell_o \mathcal{L} + \ell \mathcal{I}$, respectively. As both matrices are positive definite, the eigenvalues of the product $L^{-1}R$ are all positive and real, see [35].

Theorem 3 Consider a homogeneous distribution network with the resistance per length unit r and inductance per length unit ℓ . Suppose an output resistance r_o and an output inductance ℓ_o are attached in series to each node. Assume that $\frac{r_o}{\ell_o} < \frac{r}{\ell}$. Then the network inductivity ratio is given by

$$\Psi_{\text{NIR}} = \frac{r_o \lambda_2 + r}{\ell_o \lambda_2 + \ell},$$

where λ_2 is the algebraic connectivity of the graph $\mathcal{G}(\mathcal{V}, \mathcal{E}, \Gamma)$.

Proof: The homogeneous solution is

$$\begin{aligned} I(t) &= e^{-(r_o \mathcal{L} + r \mathcal{I})(\ell_o \mathcal{L} + \ell \mathcal{I})^{-1} t} I_0 \\ &= e^{-\mathcal{U}(r_o \Lambda + r \mathcal{I}) \mathcal{U}^T (\mathcal{U}(\ell_o \Lambda + \ell \mathcal{I}) \mathcal{U}^T)^{-1} t} I_0 \\ &= \mathcal{U} e^{-(r_o \Lambda + r \mathcal{I})(\ell_o \Lambda + \ell \mathcal{I})^{-1} t} \mathcal{U}^T I_0 \\ &= \begin{bmatrix} \frac{1}{\sqrt{n}} \mathbf{1} & \tilde{\mathcal{U}} \end{bmatrix} e^{-\begin{bmatrix} \frac{r}{\ell} & 0 \\ 0_{(n-1) \times 1} & \tilde{\Lambda}^{-1} \end{bmatrix} t} \begin{bmatrix} \frac{1}{\sqrt{n}} \mathbf{1}^T \\ \tilde{\mathcal{U}}^T \end{bmatrix} I_0, \end{aligned}$$

where $\tilde{\Lambda} = \text{diag}\{\frac{r_o \lambda_2 + r}{\ell_o \lambda_2 + \ell}, \dots, \frac{r_o \lambda_n + r}{\ell_o \lambda_n + \ell}\}$ and $0 < \lambda_2 < \lambda_3 < \dots < \lambda_n$ are nonzero eigenvalues of the admittance matrix \mathcal{L} . Note that again $\mathbf{1}^T I_0 = 0$. Similar to the proof of Theorem 1 we obtain

$$I(t, I_0) = \sum_{i=1}^{n-1} \alpha_i e^{-\frac{r_o \lambda_i + r}{\ell_o \lambda_i + \ell} t} \tilde{\mathcal{U}}_i.$$

Since $\frac{r_o}{\ell_o} < \frac{r}{\ell}$, we have

$$\frac{r_o \lambda_2 + r}{\ell_o \lambda_2 + \ell} \leq \frac{r_o \lambda_i + r}{\ell_o \lambda_i + \ell}, \quad \forall i.$$

Therefore, by Definition 1, $\Psi_{\text{NIR}} = \frac{r_o \lambda_2 + r}{\ell_o \lambda_2 + \ell}$. \blacksquare

Remark 3 In case $\frac{r_o}{\ell_o} > \frac{r}{\ell}$, the network inductivity ratio is given by

$$\Psi_{\text{NIR}} = \frac{r_o \lambda_{\max} + r}{\ell_o \lambda_{\max} + \ell},$$

where λ_{\max} is the largest eigenvalue of the Laplacian matrix of \mathcal{G} . Furthermore, if $\frac{r_o}{\ell_o} = \frac{r}{\ell}$, then $\tilde{\Lambda} = \frac{r}{\ell} \mathcal{I}$ and $\Psi_{\text{NIR}} = \frac{r}{\ell}$. However, the condition $\frac{r_o}{\ell_o} < \frac{r}{\ell}$ assumed in Theorem 3 is more relevant since the resistance r_o of the inductive output impedance is typically small. \square

Recall that the notion of network inductivity ratio allows us to quantify the inductivity behavior of the network, while the reduced model (11), in general, cannot be synthesized with RL elements only. A notable special case where the model (11) can be realized with RL elements is a complete graph with identical line lengths. Interestingly, our proposed measure

matches precisely the inductance to resistance ratio of the lines of the synthesized network in this case:

Theorem 4 Consider a power distribution network with a uniform complete graph where all the edges have the length τ . Suppose that the lines have the inductance $\ell_e \in \mathbb{R}$ and resistance $r_e \in \mathbb{R}$. Attach an output inductance ℓ_o in series with a resistance r_o to each node. Then the reduced model of the augmented graph can be synthesized with a new RL network which contains distribution lines, all with the inductance $\ell_c := n\ell_o + \ell_e$ and resistance $r_c := nr_o + r_e$, where n denotes the number of nodes. Furthermore, the resulting network inductivity ratio Ψ_{NIR} is equal to $\frac{\ell_c}{r_c}$.

Proof: The nodal injected currents satisfy $rI + \ell\dot{I} = \mathcal{L}V$. In this network, $r = \frac{r_e}{\tau}$, $\ell = \frac{\ell_e}{\tau}$, and $\mathcal{L} = \frac{n}{\tau}\Pi$ where $\Pi := \mathcal{I} - \frac{1}{n}\mathbf{1}\mathbf{1}^T$. Hence,

$$r_e I + \ell_e \dot{I} = n\Pi V. \quad (12)$$

By appending the output impedance we have $V = V_o - r_o I - \ell_o \dot{I}$. Hence (12) modifies to

$$(nr_o\Pi + r_e\mathcal{I})I + (n\ell_o\Pi + \ell_e\mathcal{I})\dot{I} = n\Pi V_o,$$

which results in

$$(n\ell_o\Pi + \ell_e\mathcal{I})^{-1}(nr_o\Pi + r_e\mathcal{I})I + \dot{I} = n(n\ell_o\Pi + \ell_e\mathcal{I})^{-1}\Pi V_o.$$

Since $(n\ell_o\Pi + \ell_e\mathcal{I})^{-1} = \frac{1}{\ell_e + n\ell_o}\mathcal{I} + \frac{\ell_o}{\ell_e(\ell_e + n\ell_o)}\mathbf{1}\mathbf{1}^T$, we obtain

$$(nr_o\Pi + r_e\mathcal{I})I + (n\ell_o + \ell_e)\dot{I} = n\Pi V_o, \quad (13)$$

where we used $\mathbf{1}^T I = 0$ and $\mathbf{1}^T \Pi = 0$. Similarly we have

$$I + \ell_c(nr_o\Pi + r_e\mathcal{I})^{-1}\dot{I} = n(nr_o\Pi + r_e\mathcal{I})^{-1}\Pi V_o,$$

and $r_c I + \ell_c \dot{I} = n\Pi V_o$. This equation is analogous to (12) and corresponds to a uniform complete graph with identical line resistance $r_c = nr_o + r_e$ and inductance $\ell_c = n\ell_o + \ell_e$.

Note that the algebraic connectivity of the weighted Laplacian \mathcal{L} is $\frac{n}{\tau}$. Following directly from Theorem 3, the inductivity ratio is computed as

$$\Psi_{\text{NIR}} = \frac{\frac{n}{\tau}\ell_o + \ell}{\frac{n}{\tau}r_o + r} = \frac{\ell_c}{r_c}.$$

Remark 4 So far, we have considered loads which are connected via power converters. It is also possible to provide the same definitions and results in the case of loads modeled with constant current sinks. Consider the graph $\mathcal{G}(\mathcal{V}, \mathcal{E}, \Gamma)$ divided into source and load nodes

$$rI_S + \ell\dot{I}_S = \mathcal{L}_{SS}V_S + \mathcal{L}_{SL}V_L$$

$$rI_L + \ell\dot{I}_L = \mathcal{L}_{LS}V_S + \mathcal{L}_{LL}V_L.$$

Suppose that load nodes are attached to constant current loads $I_L = -I_L^*$. Then $-rI_L^* = \mathcal{L}_{LS}V_S + \mathcal{L}_{LL}V_L$ and therefore $-r\mathcal{L}_{LL}^{-1}I_L^* - \mathcal{L}_{LL}^{-1}\mathcal{L}_{LS}V_S = V_L$. Substituting the latter equality into the equations above yields

$$rI_S + \ell\dot{I}_S = \mathcal{L}_{\text{red}}V_S - r\mathcal{L}_{SL}\mathcal{L}_{LL}^{-1}I_L^*.$$

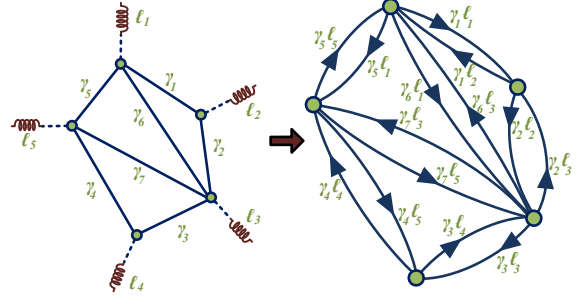


Fig. 4. Output inductances appear as weights in the corresponding directed graph, with the Laplacian $D\mathcal{L}$.

Here $\mathcal{L}_{\text{red}} = \mathcal{L}_{SS} - \mathcal{L}_{SL}\mathcal{L}_{LL}^{-1}\mathcal{L}_{LS}$ is known as the *Kron-reduced* (Laplacian) matrix derived from the Schur complement of the original Laplacian matrix \mathcal{L} [36]. Bearing in mind that $V_G = V_o - \ell_o \dot{I}_S - r_o I_S$, the system becomes

$$(r\mathcal{I} + r_o\mathcal{L}_{\text{red}})I_S + (\ell\mathcal{I} + \ell_o\mathcal{L}_{\text{red}})\dot{I}_S = \mathcal{L}_{\text{red}}V_o - r\mathcal{L}_{SL}\mathcal{L}_{LL}^{-1}I_L^*, \quad (14)$$

and one can repeat the same analysis working with \mathcal{L}_{red} instead of \mathcal{L} . Note that (14) matches the model (4) with the difference of a constant. As this constant term does not affect the homogeneous solution, the network inductivity and resistivity ratios is obtained as before. \square

D. Non-uniform Output Impedances

In this section we investigate the case where output inductances with different magnitudes are connected to the network, and we quantify the network inductivity ratio Ψ_{NIR} under this non-uniform addition. The case with non-uniform resistances can be treated in an analogous manner.

Let $D = \text{diag}(\ell_{o_1}, \ell_{o_2}, \dots, \ell_{o_n})$ where ℓ_{o_i} is the output inductance connected to the node i . We have

$$rI + \ell\dot{I} = \mathcal{L}V, \quad V = V_o - D\dot{I},$$

and hence

$$rI + (\ell\mathcal{I} + \mathcal{L}D)\dot{I} = \mathcal{L}V_o. \quad (15)$$

Note that $\mathcal{L}D$ is similar to $D^{\frac{1}{2}}\mathcal{L}D^{\frac{1}{2}}$ and therefore has nonnegative real eigenvalues. In view of equation (4), here $R = r\mathcal{I}$ and $L = \ell\mathcal{I} + \mathcal{L}D$. Hence, the matrix $L^{-1}R$ possesses positive real eigenvalues, namely $\lambda_i(L^{-1}R) = r\lambda_i^{-1}(\ell\mathcal{I} + \mathcal{L}D)$.

The matrix $\mathcal{L}D$ is also similar to $D\mathcal{L}$, which can be interpreted as the Laplacian matrix of a directed connected graph noted by $\hat{\mathcal{G}}(\mathcal{V}, \hat{\mathcal{E}}, \hat{\Gamma})$ with the same nodes as the original graph $\mathcal{V} = \{1, \dots, n\}$, and directed edges $\hat{\mathcal{E}} \subset \mathcal{V} \times \mathcal{V}$. As shown in figure 4, in this representation, for any node pair $(i, j) \in \hat{\mathcal{E}}$, there exists a directed edge from node i to node j with the weight $D_i\tau_{ij}^{-1}$ (recall that τ_{ij}^{-1} is the weight of the edge $\{i, j\} \in \mathcal{E}$ of the original graph \mathcal{G}). Note that the edge set $\hat{\mathcal{E}}$ is symmetric meaning that $(i, j) \in \hat{\mathcal{E}} \Leftrightarrow (j, i) \in \hat{\mathcal{E}}$, and its cardinality is equal to $2m$. We take advantage of this graph to obtain the network inductivity ratio Ψ_{NIR} , as formalized in the following theorem.

Theorem 5 Consider a homogeneous distribution network with the resistance per length unit r , inductance per length unit ℓ , edge lengths τ_1, \dots, τ_n , and output inductors $\ell_{o_1}, \ell_{o_2}, \dots, \ell_{o_n}$. Then the network inductivity ratio is given by

$$\Psi_{\text{NIR}} = \frac{\lambda_2 + \ell}{r},$$

where λ_2 is the algebraic connectivity of the graph $\hat{\mathcal{G}}(\mathcal{V}, \hat{\mathcal{E}}, \hat{\Gamma})$ defined above.

Proof: Let $\mathcal{L}' = D^{\frac{1}{2}} \mathcal{L} D^{\frac{1}{2}}$. The homogeneous solution to (15) is

$$\begin{aligned} I(t) &= e^{-r(\ell\mathcal{I} + \mathcal{L}D)^{-1}t} I_0 = D^{-\frac{1}{2}} e^{-rD^{\frac{1}{2}}(\ell\mathcal{I} + \mathcal{L}D)^{-1}D^{-\frac{1}{2}}t} D^{\frac{1}{2}} I_0 \\ &= D^{-\frac{1}{2}} e^{-r(\ell\mathcal{I} + \mathcal{L}')^{-1}t} D^{\frac{1}{2}} I_0. \end{aligned}$$

Note that \mathcal{L}' is positive semi-definite and thus $\ell\mathcal{I} + \mathcal{L}'$ is invertible. Bearing in mind that 0 is an eigenvalue of the matrix \mathcal{L}' with the corresponding normalized eigenvector $\mathcal{U}_1 = (\mathbb{1}^T D^{-1} \mathbb{1})^{-\frac{1}{2}} D^{-\frac{1}{2}} \mathbb{1}$, and by the spectral decomposition $\mathcal{L}' = \mathcal{U} \Lambda \mathcal{U}^T$, we find that

$$\begin{aligned} I(t) &= D^{-\frac{1}{2}} e^{-r(\mathcal{U}(\ell\mathcal{I} + \Lambda)\mathcal{U}^T)^{-1}t} D^{\frac{1}{2}} I_0 \\ &= D^{-\frac{1}{2}} \mathcal{U} e^{-r(\ell\mathcal{I} + \Lambda)^{-1}t} \mathcal{U}^T D^{\frac{1}{2}} I_0 \\ &= D^{-\frac{1}{2}} [\mathcal{U}_1 \quad \tilde{\mathcal{U}}] e^{-r \begin{bmatrix} \frac{1}{\ell} & 0 \\ 0_{(n-1) \times 1} & \tilde{\Lambda}^{-1} \end{bmatrix} t} \begin{bmatrix} \mathcal{U}_1^T \\ \tilde{\mathcal{U}}^T \end{bmatrix} D^{\frac{1}{2}} I_0, \end{aligned}$$

where $\tilde{\Lambda} = \text{diag}\{\lambda_2 + \ell, \lambda_3 + \ell, \dots, \lambda_n + \ell\}$ and $0 < \lambda_2 < \lambda_3 < \dots < \lambda_n$ are nonzero eigenvalues of the matrix \mathcal{L}' . Let $\tilde{I}(t) = D^{\frac{1}{2}} I(t)$. Noting that by the Kirchhoff Law, $\mathbb{1}^T I_0 = 0$, we have

$$\tilde{I}(t) = \tilde{\mathcal{U}} e^{-r\tilde{\Lambda}^{-1}t} \tilde{\mathcal{U}}^T \tilde{I}_0.$$

Since $\mathcal{U}_1^T \tilde{I}_0 = 0$ we can write \tilde{I}_0 as the linear combination $\tilde{I}_0 = \tilde{\mathcal{U}} X$, $X \in \mathbb{R}^{(n-1) \times 1}$. Now we have

$$\tilde{I}(t) = \tilde{\mathcal{U}} e^{-r\tilde{\Lambda}^{-1}t}, \quad \|\tilde{I}(t)\|^2 = X^T e^{-2r\tilde{\Lambda}^{-1}t} X.$$

Hence

$$\begin{aligned} \|\tilde{I}(t)\|^2 &\geq e^{-\frac{2r}{\lambda_2 + \ell}t} \|\tilde{I}_0\|^2, \quad I^T(t) D I(t) \geq e^{-\frac{2r}{\lambda_2 + \ell}t} I_0^T D I_0, \\ \|I(t)\| &\geq \mu e^{-\frac{r}{\lambda_2 + \ell}t} \|I_0\|, \end{aligned}$$

where $\mu := \sqrt{\frac{\min_i(\ell_{o_i})}{\max_i(\ell_{o_i})}}$.

This yields $\Psi_{\text{NIR}} = \frac{\lambda_2 + \ell}{r}$. Note that the eigenvalues of \mathcal{L}' and $D\mathcal{L}$ are the same. This completes the proof. ■

Remark 5 Utilizing the results of [37], since the \mathcal{L} and D are both positive semi-definite matrices, we have

$$\min_i(\ell_{o_i}) \lambda_2(\mathcal{L}) \leq \lambda_2(D\mathcal{L}) \leq \max_i(\ell_{o_i}) \lambda_2(\mathcal{L}). \quad (16)$$

These bounds can be used to ensure that the network inductivity ratio lies within certain values, without explicitly calculating the algebraic connectivity of the directed graph associated with the Laplacian $D\mathcal{L}$. □

Remark 6 The algebraic connectivity of the network can be estimated through distributed methods in both undirected [38],

[39], and directed graphs [40]. Furthermore, line parameters (resistance and inductance) can be identified through PMUs (Phase Measurement Units) [41] [42] [43]. Therefore, our proposed measure can be calculated in a distributed manner and the network can be expanded arbitrarily where no central control unit is required. □

III. OPTIMIZING THE NETWORK INDUCTIVITY RATIO

The results proposed in the previous sections can be also exploited to maximize the diffusion of output impedances into the network. We address this problem by maximizing the network inductivity ratio of the network for both uniform and non-uniform output impedances.

A. Optimization for Networks with Uniform Output Impedances

Here, we formalize the problem of maximizing the network inductivity ratio given output inductances and the topology of the graph. The decision variables are the distances between nodes which should be designed such that the network inductivity ratio is maximized. By Theorem 1, this is equivalent to maximizing the algebraic connectivity of the graph $\mathcal{G}(\mathcal{V}, \mathcal{E}, \Gamma)$, where $\Gamma = \text{diag}(\gamma)$ is given by (2). The algebraic connectivity can be formulated as

$$\begin{aligned} \lambda_2(\gamma) &= \min_{\|v\|=1, \mathbb{1}^T v=0} v^T \mathcal{L}(\gamma) v \\ &= \min_{\|v\|=1, \mathbb{1}^T v=0} \sum_{\{i,j\} \in \mathcal{E}} \gamma_k (v_i - v_j)^2, \quad k \sim \{i, j\} \end{aligned}$$

The equality above shows that $\lambda_2(\gamma)$ is the pointwise minimum of a summation of linear functions of γ and hence $\lambda_2(\gamma)$ is a concave function of γ [44]. Therefore maximization of the algebraic connectivity of a network with tunable distribution line lengths is a convex optimization problem under a linear constraint such as

$$\sum_{\{i,j\} \in \mathcal{E}} c_{ij} \gamma_{ij} \leq 1,$$

where $c \in \mathbb{R}^{n \times n}$ is associated with the relative cost of the edge $\{i, j\}$. This problem can be cast into a Semidefinite Program (SDP) formulation [45].

B. Optimization for Networks with Non-Uniform Output Impedances

We aim to optimize the distribution of the inductors among sources such that the maximum network inductivity ratio is achieved. We assume that we have limited resources of inductors, which is reflected in the following ‘‘budget constraint’’:

$$\sum_i \ell_{o_i} \leq c, \quad c \in \mathbb{R}^+. \quad (17)$$

According to Theorem 5, this problem is equivalent to maximizing the algebraic connectivity of the directed graph $\hat{\mathcal{G}}$ under the budget constraint. The algebraic connectivity can be written as

$$\lambda_2(\hat{\mathcal{G}}) = \min_{v \neq 0, v^T D^{-\frac{1}{2}} \mathbb{1} = 0} \frac{v^T D^{\frac{1}{2}} \mathcal{L} D^{\frac{1}{2}} v}{\|v\|}.$$

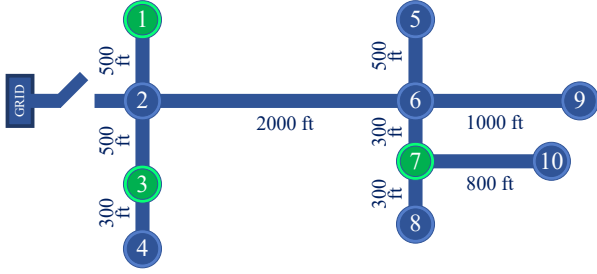


Fig. 5. Schematic of the islanded IEEE 13 node test feeder graph. Power sources are connected to the (green) nodes 1, 3, and 7.

By defining $u := D^{-\frac{1}{2}}v$, the optimization problem can be restated as follows:

$$\max_D \min_{u \neq 0, u^T \mathbf{1} = 0} \frac{u^T D \mathcal{L} D u}{\|D^{\frac{1}{2}} u\|^2} \quad \text{s.t.} \quad \text{trace}(D) \leq c. \quad (18)$$

Below we provide examples where we opt for maximizing the network inductivity ratio for specific network topologies.

1) *IEEE 13 Node Test Feeder*: Figure 5 depicts the graph of the islanded IEEE 13 node test feeder. Here, all the distribution lines are assumed to have the same reactance per length equal to $\omega \ell = 1.2 \frac{\Omega}{\text{mile}}$ and resistance per length equal to $r = 0.7 \frac{\Omega}{\text{mile}}$, derived from the configuration 602 [46]. We consider the case where three inverters are connected to the nodes 1, 3, and 7, and the rest of the nodes are connected to constant current loads. After carrying out Kron reduction, the algebraic connectivity of the resulting Laplacian is equal to 3.1. To be able to quantify the changes in line phase angles after addition of output impedances, we define θ_{NIR} as

$$\theta_{\text{NIR}} := \arctan(\omega \Psi_{\text{NIR}}). \quad (19)$$

Note that, before adding the output inductances, $\theta_{\text{NIR}} = \arctan \frac{\omega \ell}{r} = \frac{2\pi}{3}$. Using results of Theorem 1, for a 10% increase in θ_{NIR} , a uniform inductor of 3.21mH should be attached to all of the sources output. However, if the nodes possess different values of output inductors, by using the result of Theorem 5, the same increase in the network inductivity ratio can be achieved optimally with 0.95mH, 0.95mH, and 4.35mH inductors, for the nodes 1, 3, and 7 respectively. This is feasible in practice since the typical values for inverter output filter inductance and implemented output virtual inductance range from 0.5mH to 50mH [3], [4], [14], [21], [22], [27], [47]–[51].

2) *Star Graph*: Consider the graph \mathcal{G} with the Laplacian \mathcal{L} , consisting of four nodes in a star topology. The line lengths are 5pu, 7pu, and 9pu, as depicted in Figure 6. Note that here again, the weights of the edges are the inverse of the distances. Attach the output impedances $D = \text{diag}\{\ell_1, \ell_2, \ell_3, \ell_4\}$, and for simplicity, assume that the budget constraint (17) holds with equality. Hence $\ell_4 = c - (\ell_1 + \ell_2 + \ell_3)$. Figure 6 shows different values of the second smallest eigenvalue of the matrix $D\mathcal{L}$. We obtain that the maximum algebraic connectivity is achieved when no output impedance is used (wasted) for the node in the middle. Interestingly, optimal values for output inductors are proportional to the node's distance to the middle node.

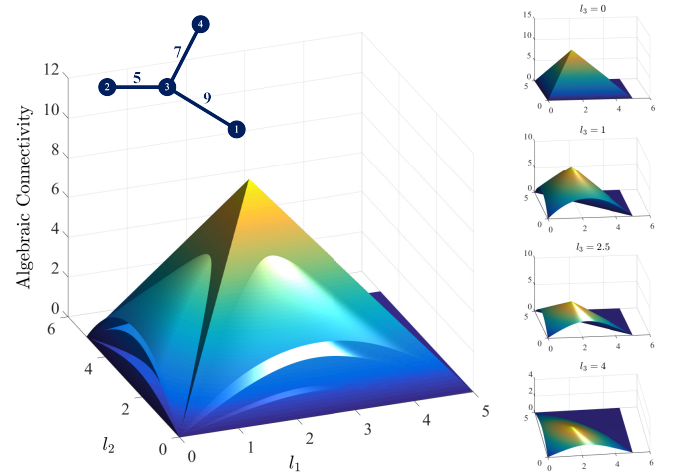


Fig. 6. Algebraic connectivity of the directed graph associated with the Laplacian $D\mathcal{L}$, where \mathcal{L} is the Laplacian of the star graph shown in dark blue. The budget constraint is $\sum_i \ell_i = c = 5\text{mH}$. On the right, the algebraic connectivity is plotted as a function of ℓ_1 and ℓ_2 for different values of ℓ_3 . Note that $\ell_4 = c - \ell_1 - \ell_2 - \ell_3$. On the left, all the four subplots are merged. Clearly, the optimal algebraic connectivity is achieved where no output impedance is used for node 3 (the middle node), and $\ell_1 = 2.20\text{mH}$, $\ell_2 = 1.23\text{mH}$, $\ell_4 = 1.57\text{mH}$ are used for nodes 1, 2, and 4 respectively.

3) *Networks with Internal Constant Voltage Buses*: Recall the grid represented by the undirected graph $\mathcal{G}(\mathcal{V}, \mathcal{E}, \Gamma)$. Here, we bisect the nodes $\mathcal{V} = \{1, \dots, n\}$ into sources $\mathcal{V}_S = \{1, \dots, n_S\}$, and constant voltage buses $\mathcal{V}_B = \{n_S+1, \dots, n_S+n_B\}$, and assume that the source nodes are not directly connected to each other but through the buses. A commonly-used example for such an architecture is the network of power converters connected to a common bus node. The electrical distribution network with this topology is referred to as *Parallel Microgrid* [52], and has been investigated in large number of articles (see e.g. [53]–[61]).

We can decompose the Laplacian \mathcal{L} as

$$\mathcal{L} = \begin{bmatrix} \mathcal{L}_{SS} & \mathcal{L}_{SB} \\ \mathcal{L}_{BS} & \mathcal{L}_{BB} \end{bmatrix}.$$

Note that \mathcal{L}_{SS} is diagonal. We have $V_S = V_o - D\dot{I}_S$, where $V_o \in \mathbb{R}^{n_S}$ and $V_S \in \mathbb{R}^{n_S}$ represent the voltages of the sources and the voltages at the end of the output inductors respectively. Hence

$$r\dot{I}_S + (\ell\mathcal{I} + \mathcal{L}_{SS}D)\dot{I}_S = \mathcal{L}_{SS}V_o + \mathcal{L}_{SB}V_B^*, \quad (20)$$

where $V_B^* \in \mathbb{R}^{n_B}$ is the constant vector of the bus voltages.

Theorem 6 Consider a homogeneous distribution network with the resistance per length unit r , inductance per length unit ℓ , and output inductors $\ell_{o_1}, \ell_{o_2}, \dots, \ell_{o_{n_S}}$ connected to all the n_S inverters. Assume that the inverters are not directly interconnected with each other but through constant voltage buses, and the sum of output inductors satisfies (17). Then the maximum network inductivity ratio is

$$\Psi_{\text{NIR}} = r^{-1} \left(\ell + \sum_i \frac{c}{\tau_i} \right),$$

with the optimal output impedances

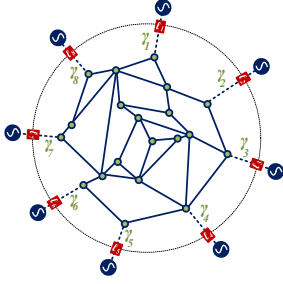


Fig. 7. Schematic of a network topology where the sources are connected to each other through internal nodes. The optimized values for output inductors (ℓ_i) are proportional to the distance between the source and the nearest bus node ($\tau_i = \gamma_i^{-1}$).

$$\ell_{o_i} = \frac{\tau_i}{\sum_i \tau_i} c, \quad (21)$$

where $\tau_i = \gamma_i^{-1}$ is the distance of the source i to the connected internal node (see figure 7).

Proof: We have the homogeneous solution

$$I_S(t) = e^{-r(\ell\mathcal{I} + \mathcal{L}_{SS}D)^{-1}t} I_{S_0}$$

Note that $\mathcal{L}_{SS}D$ is a diagonal matrix, and let ρ denote its minimum diagonal element, i.e., $\rho := \min_i (\mathcal{L}_{SS}D)_{ii}$. The equality above yields

$$\|I_S(t)\| \geq e^{-\frac{r}{\rho+t}t} \|I_{S_0}\|,$$

and thus $\Psi_{\text{NIR}} = \frac{\rho+t}{r}$. Note that here, since $\mathbb{1}^T I_S \neq 0$, we calculate the smallest eigenvalue of $\mathcal{L}_{SS}D$ instead of the algebraic connectivity of \mathcal{L} . Due to the budget constraint (17) and noting that $\mathcal{L}_{SS} = \text{diag}\{\tau_1^{-1}, \dots, \tau_{n_S}^{-1}\}$, the choice of $\ell_{o_i} = \frac{\tau_i}{\sum_i \tau_i} c$ maximizes the network inductivity, with the corresponding value of Ψ_{NIR} specified in the theorem. ■

Remark 7 In case source i is connected to multiple internal buses, τ_i in (21) should be replaced with τ'_i defined as

$$\tau'_i := \left(\sum_{j \in \mathcal{N}_i} \tau_k^{-1} \right)^{-1}, \quad k \sim \{i, j\},$$

where \mathcal{N}_i denotes all the internal nodes connected to i^{th} source node. □

IV. KRON REDUCTION IN PHASOR DOMAIN AND THE PROPOSED MEASURE

As depicted in Figure 8, Kron reduction in the phasor domain provides the model for the augmented nodes. Note that, in the Kron reduced model, some of the edges coincide with the lines of the original network into which the output impedances were diffused, while others (dotted green) are created as a result of the Kron reduction. We refer to these edges as *physical* and *virtual* lines, respectively. The Kron reduction does not necessarily preserve the homogeneity of the distribution lines, and hence except in some special cases, the equation (3) is not valid for the reduced network. However, the reduced model can still be expressed by complex numbers in phasor domain, and the corresponding line angles can be

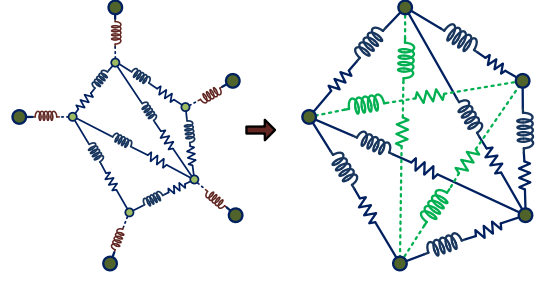


Fig. 8. Kron reduction of an arbitrary graph with added output impedances.

used to validate our proposed inductivity metrics. To this end, we first write the currents of the edges as

$$\begin{bmatrix} I \\ 0 \end{bmatrix} = \begin{bmatrix} y_o \mathcal{I} & -y_o \mathcal{I} \\ -y_o \mathcal{I} & y_o \mathcal{I} + y_\ell \mathcal{L} \end{bmatrix} \begin{bmatrix} V_o \\ V \end{bmatrix},$$

where $y_o = \frac{1}{j\omega\ell_o}$, $y_\ell = \frac{1}{r+j\omega\ell}$. The Kron-reduced model then reads as

$$\mathcal{Y}_{\text{red}} = y_o [\mathcal{I} - (\mathcal{I} + \frac{y_\ell}{y_o} \mathcal{L})^{-1}]. \quad (22)$$

Since the graph of the inner nodes is connected, the resulting Kron-reduced network is always a complete graph [62].

Below we provide several numerical examples for the case of uniform output inductances added to the network. In these examples, for the sake of clarity of the figures, we compare the line phase angles

$$\theta_{ij} := \arctan \frac{\text{Im}(1/\mathcal{Y}_{\text{red}ij})}{\text{Re}(1/\mathcal{Y}_{\text{red}ij})}$$

for the line $\{i, j\}$, with θ_{NIR} as defined in (19). Here we let $\omega = 1$, for simplicity. As will be observed, our numerical investigation shows that compared to the physical lines, the virtual lines respond much slower to the increase in the inductive output impedance. Hence the less virtual lines the reduced graph contains, the more output impedance diffuses in the network, which is consistent with Remark 1.

A. Complete nonuniform graphs

Here, we consider a 4-node complete graph with different distribution line lengths. As it is shown in Figure 9, the proposed measure matches with the overall behavior of the line angles as the added output inductance increases.

B. Cycle uniform graphs

Algebraic connectivity of a uniform cycle graph is $2(1 - \cos \frac{2\pi}{n})$, which can be used to calculate Ψ_{NIR} . As can be seen in Figure 10, the phase angle of virtual edges, θ_{13} and θ_{24} , are less affected by the addition of the output inductances.

C. Path uniform graphs

The algebraic connectivity of a uniform path graph is $2(1 - \cos \frac{\pi}{n})$. Figure 11 depicts the changes in θ_{ij} s as the output inductance increases. In this case, the inductance and resistance possess negative values at some edges for certain values of the output impedance. Therefore, the Kron reduced phasor model fails to provide a meaningful inductivity ratio

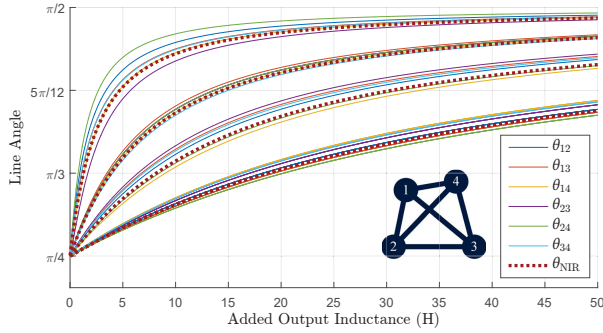


Fig. 9. The original graph is a complete nonuniform graph (dark blue). Phase angles of the distribution lines after Kron reduction follows the behavior exerted by the proposed measure. The initial phase angle of the lines is $\frac{\pi}{4}$ and the lengths are as follows: $[\tau_{12}, \tau_{13}, \tau_{14}, \tau_{23}, \tau_{24}, \tau_{34}] =$ (a) $[5, 6, 9, 7, 4, 6]$; (b) $[20, 19, 20, 21, 20, 22]$; (c) $[40, 37, 35, 49, 46, 38]$; (d) $[100, 105, 93, 87, 110, 89]$

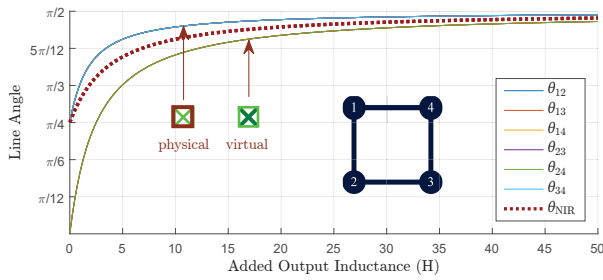


Fig. 10. Line angles of the Kron-reduced model of a cycle graph (dark blue) with added output inductances. The initial phase angle of the lines is $\frac{\pi}{4}$.

for those edges. On the contrary, the proposed inductivity measure remains within the physically meaningful interval $\arctan(\Psi_{\text{NIR}}) \in [0, \pi/2]$. Similar to the case of cycle graph, the virtual edges diminish the impact of the added output inductors.

V. CONCLUSION

In this paper the influence of the output impedance on the inductivity and resistivity of the distribution lines has been investigated. Two measures, network inductivity ratio and network resistivity ratio, were proposed and analyzed without relying on the pure sinusoidal signals assumption (phasors). The analysis revealed the fact that the more connected the graph is, the more output impedance diffuses into the network and the larger its effect will be. We have studied how the

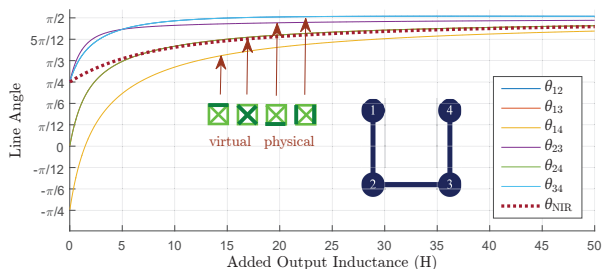


Fig. 11. Line angles of the Kron-reduced model of a path graph (dark blue) with added output inductances. The line initial angle is $\frac{\pi}{4}$.

impact of inductive output impedances on the network can be maximized in specific network topologies. We compared the proposed measure to the phase angles of the lines of a phasor-based Kron reduced network. Results confirm the validity and effectiveness of the proposed metrics. Future works include investigating analytical solutions maximizing the network inductivity/resistivity ratios in more general topologies and incorporating different load models in the proposed scheme.

REFERENCES

- [1] D. E. Olivares, A. Mehrizi-Sani, A. H. Etemadi, C. A. Caizares, R. Iravani, M. Kazerani, A. H. Hajimiragha, O. Gomis-Bellmunt, M. Saeedifard, R. Palma-Behnke, G. A. Jimenez-Estvez, and N. D. Hatziargyriou, "Trends in microgrid control," *IEEE Transactions on Smart Grid*, vol. 5, no. 4, pp. 1905–1919, July 2014.
- [2] J. M. Guerrero, L. G. De Vicuna, J. Matas, M. Castilla, and J. Miret, "Output impedance design of parallel-connected ups inverters with wireless load-sharing control," *IEEE Transactions on industrial electronics*, vol. 52, no. 4, pp. 1126–1135, 2005.
- [3] J. M. Guerrero, J. Matas, L. G. D. V. De Vicuna, M. Castilla, and J. Miret, "Wireless-control strategy for parallel operation of distributed-generation inverters," *IEEE Transactions on Industrial Electronics*, vol. 53, no. 5, pp. 1461–1470, 2006.
- [4] J. M. Guerrero, J. Matas, L. G. de Vicuna, M. Castilla, and J. Miret, "Decentralized control for parallel operation of distributed generation inverters using resistive output impedance," *IEEE Transactions on industrial electronics*, vol. 54, no. 2, pp. 994–1004, 2007.
- [5] J. M. Guerrero, J. C. Vasquez, J. Matas, M. Castilla, and L. G. de Vicuña, "Control strategy for flexible microgrid based on parallel line-interactive ups systems," *IEEE Transactions on Industrial Electronics*, vol. 56, no. 3, pp. 726–736, 2009.
- [6] J. Guerrero, P. Loh, M. Chandorkar, and T. Lee, "Advanced control architectures for intelligent microgrids - Part I: Decentralized and hierarchical control," *IEEE Transactions Industrial Electronics*, no. 99, pp. 1–1, 2013.
- [7] J. Schiffer, R. Ortega, A. Astolfi, J. Raisch, and T. Sezi, "Conditions for stability of droop-controlled inverter-based microgrids," *Automatica*, vol. 50, no. 10, pp. 2457 – 2469, 2014.
- [8] C. De Persis and N. Monshizadeh, "Bregman storage functions for microgrid control," *arXiv preprint ArXiv:1510.05811*, 2015.
- [9] N. Monshizadeh and C. D. Persis, "Output agreement in networks with unmatched disturbances and algebraic constraints," in *2015 54th IEEE Conference on Decision and Control (CDC)*, Dec 2015, pp. 4196–4201.
- [10] C. D. Persis, N. Monshizadeh, J. Schiffer, and F. Dörfler, "A Lyapunov approach to control of microgrids with a network-preserved differential-algebraic model," in *2016 IEEE 55th Conference on Decision and Control (CDC)*, Dec 2016, pp. 2595–2600.
- [11] N. Monshizadeh and C. D. Persis, "Agreeing in networks: Unmatched disturbances, algebraic constraints and optimality," *Automatica*, vol. 75, pp. 63 – 74, 2017.
- [12] N. Tsolas, A. Arapostathis, and P. Varaiya, "A structure preserving energy function for power system transient stability analysis," *IEEE Transactions on Circuits and Systems*, vol. 32, no. 10, pp. 1041–1049, Oct 1985.
- [13] J. Rocabert, A. Luna, F. Blaabjerg, and P. Rodriguez, "Control of power converters in AC microgrids," *Power Electronics, IEEE Transactions on*, vol. 27, no. 11, pp. 4734–4749, Nov 2012.
- [14] Y. W. Li and C. N. Kao, "An accurate power control strategy for power-electronics-interfaced distributed generation units operating in a low-voltage multibus microgrid," *IEEE Transactions on Power Electronics*, vol. 24, no. 12, pp. 2977–2988, Dec 2009.
- [15] J. W. Simpson-Porco, F. Dörfler, and F. Bullo, "Synchronization and power sharing for droop-controlled inverters in islanded microgrids," *Automatica*, vol. 49, no. 9, pp. 2603 – 2611, 2013.
- [16] J. Schiffer, T. Seel, J. Raisch, and T. Sezi, "Voltage stability and reactive power sharing in inverter-based microgrids with consensus-based distributed voltage control," *IEEE Transactions on Control Systems Technology*, vol. 24, no. 1, pp. 96–109, 2016.
- [17] A. Engler, "Applicability of droops in low voltage grids," *DER J.*, vol. 1, pp. 1–5, 2005.
- [18] X. Yu, A. M. Khambadkone, H. Wang, and S. T. S. Terence, "Control of parallel-connected power converters for low-voltage microgrid – Part I: A hybrid control architecture," *IEEE Transactions on Power Electronics*, vol. 25, no. 12, pp. 2962–2970, Dec 2010.

- [19] H. Mahmood, D. Michaelson, and J. Jiang, "Accurate reactive power sharing in an islanded microgrid using adaptive virtual impedances," *IEEE Transactions on Power Electronics*, vol. 30, no. 3, pp. 1605–1617, March 2015.
- [20] R. Moslemi, J. Mohammadpour, and A. Mesbahi, "A modified droop control for reactive power sharing in large microgrids with meshed topology," in *2016 American Control Conference (ACC)*, July 2016, pp. 6779–6784.
- [21] K. D. Brabandere, B. Bolsens, J. V. den Keybus, A. Woyte, J. Driesen, and R. Belmans, "A voltage and frequency droop control method for parallel inverters," *IEEE Transactions on Power Electronics*, vol. 22, no. 4, pp. 1107–1115, July 2007.
- [22] J. Matas, M. Castilla, L. G. de Vicua, J. Miret, and J. C. Vasquez, "Virtual impedance loop for droop-controlled single-phase parallel inverters using a second-order general-integrator scheme," *IEEE Transactions on Power Electronics*, vol. 25, no. 12, pp. 2993–3002, Dec 2010.
- [23] S. J. Chiang, C. Y. Yen, and K. T. Chang, "A multimodule parallel-series-connected PWM voltage regulator," *IEEE Transactions on Industrial Electronics*, vol. 48, no. 3, pp. 506–516, Jun 2001.
- [24] J. Guerrero, L. Hang, and J. Uceda, "Control of distributed uninterruptible power supply systems," *Industrial Electronics, IEEE Transactions on*, vol. 55, no. 8, pp. 2845–2859, Aug 2008.
- [25] W. Yao, M. Chen, J. Matas, J. M. Guerrero, and Z. M. Qian, "Design and analysis of the droop control method for parallel inverters considering the impact of the complex impedance on the power sharing," *IEEE Transactions on Industrial Electronics*, vol. 58, no. 2, pp. 576–588, Feb 2011.
- [26] D. M. Vilathgamuwa, P. C. Loh, and Y. Li, "Protection of microgrids during utility voltage sags," *IEEE Transactions on Industrial Electronics*, vol. 53, no. 5, pp. 1427–1436, Oct 2006.
- [27] J. Kim, J. M. Guerrero, P. Rodriguez, R. Teodorescu, and K. Nam, "Mode adaptive droop control with virtual output impedances for an inverter-based flexible AC microgrid," *IEEE Transactions on Power Electronics*, vol. 26, no. 3, pp. 689–701, March 2011.
- [28] A. van der Schaft, "Characterization and partial synthesis of the behavior of resistive circuits at their terminals," *Systems & Control Letters*, vol. 59, no. 7, pp. 423–428, 2010.
- [29] E. I. Verriest and J. C. Willems, "The behavior of linear time invariant RLC circuits," in *49th IEEE Conference on Decision and Control (CDC)*, Dec 2010, pp. 7754–7758.
- [30] S. Y. Caliskan and P. Tabuada, "Kron reduction of power networks with lossy and dynamic transmission lines," in *2012 IEEE 51st IEEE Conference on Decision and Control (CDC)*, Dec 2012, pp. 5554–5559.
- [31] S. Y. Caliskan and P. Tabuada, "Towards kron reduction of generalized electrical networks," *Automatica*, vol. 50, no. 10, pp. 2586–2590, 2014.
- [32] A. Teixeira, K. Paridari, H. Sandberg, and K. H. Johansson, "Voltage control for interconnected microgrids under adversarial actions," in *2015 IEEE 20th Conference on Emerging Technologies & Factory Automation (ETFA)*. IEEE, 2015, pp. 1–8.
- [33] B. Mohar, "Laplace eigenvalues of graphs survey," *Discrete Mathematics*, vol. 109, no. 13, pp. 171–183, 1992.
- [34] N. M. M. De Abreu, "Old and new results on algebraic connectivity of graphs," *Linear algebra and its applications*, vol. 423, no. 1, pp. 53–73, 2007.
- [35] R. A. Horn and C. R. Johnson, *Matrix Analysis*. Cambridge university press, 2012.
- [36] G. Kron, *Tensor Analysis of Networks*, 1939.
- [37] J. K. Merikoski and R. Kumar, "Inequalities for spreads of matrix sums and products," in *Applied Mathematics E-Notes*, 4:150–159, 2004.
- [38] M. Franceschelli, A. Gasparri, A. Giua, and C. Seatzu, "Decentralized Laplacian eigenvalues estimation for networked multi-agent systems," in *Decision and Control, 2009 held jointly with the 2009 28th Chinese Control Conference. CDC/CCC 2009. Proceedings of the 48th IEEE Conference on*, Dec 2009, pp. 2717–2722.
- [39] P. D. Lorenzo and S. Barbarossa, "Distributed estimation and control of algebraic connectivity over random graphs," *IEEE Transactions on Signal Processing*, vol. 62, no. 21, pp. 5615–5628, Nov 2014.
- [40] C. Li and Z. Qu, "Distributed estimation of algebraic connectivity of directed networks," *Systems & Control Letters*, vol. 62, no. 6, pp. 517–524, 2013.
- [41] X. Zhao, H. Zhou, D. Shi, H. Zhao, C. Jing, and C. Jones, "On-line PMU-based transmission line parameter identification," *CSEE Journal of Power and Energy Systems*, vol. 1, no. 2, pp. 68–74, June 2015.
- [42] Y. Du and Y. Liao, "On-line estimation of transmission line parameters, temperature and sag using PMU measurements," *Electric Power Systems Research*, vol. 93, pp. 39–45, 2012.
- [43] D. Shi, D. J. Tylavsky, K. M. Koellner, N. Logic, and D. E. Wheeler, "Transmission line parameter identification using PMU measurements," *European Transactions on Electrical Power*, vol. 21, no. 4, pp. 1574–1588, 2011.
- [44] S. Boyd and L. Vandenberghe, *Convex Optimization*. Cambridge University Press, 2004.
- [45] J. Sun, S. Boyd, L. Xiao, and P. Diaconis, "The fastest mixing markov process on a graph and a connection to a maximum variance unfolding problem," *SIAM review*, vol. 48, no. 4, pp. 681–699, 2006.
- [46] Distribution System Analysis Subcommittee, "IEEE 13 Node Test Feeder," *IEEE Power Engineering Society, Power System Analysis, Computing and Economics Committee*.
- [47] J. He, Y. W. Li, D. Bosnjak, and B. Harris, "Investigation and active damping of multiple resonances in a parallel-inverter-based microgrid," *IEEE Transactions on Power Electronics*, vol. 28, no. 1, pp. 234–246, Jan 2013.
- [48] J. He and Y. W. Li, "Generalized closed-loop control schemes with embedded virtual impedances for voltage source converters with LC or LCL filters," *IEEE Transactions on Power Electronics*, vol. 27, no. 4, pp. 1850–1861, April 2012.
- [49] J. M. Guerrero, J. C. Vasquez, J. Matas, L. G. de Vicuna, and M. Castilla, "Hierarchical control of droop-controlled AC and DC microgrids; a general approach toward standardization," *IEEE Transactions on Industrial Electronics*, vol. 58, no. 1, pp. 158–172, Jan 2011.
- [50] Y. A. R. I. Mohamed and E. F. El-Saadany, "Adaptive decentralized droop controller to preserve power sharing stability of paralleled inverters in distributed generation microgrids," *IEEE Transactions on Power Electronics*, vol. 23, no. 6, pp. 2806–2816, Nov 2008.
- [51] J. He and Y. W. Li, "Analysis, design, and implementation of virtual impedance for power electronics interfaced distributed generation," *IEEE Transactions on Industry Applications*, vol. 47, no. 6, pp. 2525–2538, Nov 2011.
- [52] J. W. Simpson-Porco, F. Dorfler, and F. Bullo, "Voltage stabilization in microgrids via quadratic droop control," *IEEE Transactions on Automatic Control*, 2016.
- [53] B. B. Johnson, S. V. Dhople, A. O. Hamadeh, and P. T. Krein, "Synchronization of nonlinear oscillators in an LTI electrical power network," *IEEE Transactions on Circuits and Systems I: Regular Papers*, vol. 61, no. 3, pp. 834–844, March 2014.
- [54] J. Wang, N. C. P. Chang, X. Feng, and A. Monti, "Design of a generalized control algorithm for parallel inverters for smooth microgrid transition operation," *IEEE Transactions on Industrial Electronics*, vol. 62, no. 8, pp. 4900–4914, Aug 2015.
- [55] A. M. Roslan, K. H. Ahmed, S. J. Finney, and B. W. Williams, "Improved instantaneous average current-sharing control scheme for parallel-connected inverter considering line impedance impact in microgrid networks," *IEEE Transactions on Power Electronics*, vol. 26, no. 3, pp. 702–716, March 2011.
- [56] C. L. Chen, Y. Wang, J. S. Lai, Y. S. Lee, and D. Martin, "Design of parallel inverters for smooth mode transfer microgrid applications," *IEEE Transactions on Power Electronics*, vol. 25, no. 1, pp. 6–15, Jan 2010.
- [57] J. M. Guerrero, J. C. Vasquez, J. Matas, M. Castilla, and L. G. de Vicuna, "Control strategy for flexible microgrid based on parallel line-interactive UPS systems," *IEEE Transactions on Industrial Electronics*, vol. 56, no. 3, pp. 726–736, March 2009.
- [58] S. Dasgupta, S. K. Sahoo, and S. K. Panda, "Single-phase inverter control techniques for interfacing renewable energy sources with microgrid—Part I: Parallel-connected inverter topology with active and reactive power flow control along with grid current shaping," *IEEE Transactions on Power Electronics*, vol. 26, no. 3, pp. 717–731, March 2011.
- [59] R. O. Gonzalez, O. C. Castillo, J. C. S. Saavedra, V. H. G. Ortega, and A. G. Trejo, "Application control configurations for parallel connection of single-phase energy conversion units operating in island mode," *IEEE Latin America Transactions*, vol. 14, no. 2, pp. 694–703, Feb 2016.
- [60] T. Wu, Z. Liu, J. Liu, S. Wang, and Z. You, "A unified virtual power decoupling method for droop-controlled parallel inverters in microgrids," *IEEE Transactions on Power Electronics*, vol. 31, no. 8, pp. 5587–5603, Aug 2016.
- [61] Y. Chen, J. M. Guerrero, Z. Shuai, Z. Chen, L. Zhou, and A. Luo, "Fast reactive power sharing, circulating current and resonance suppression for parallel inverters using resistive-capacitive output impedance," *IEEE Transactions on Power Electronics*, vol. 31, no. 8, pp. 5524–5537, Aug 2016.
- [62] F. Dörfler and F. Bullo, "Kron reduction of graphs with applications to electrical networks," *IEEE Transactions on Circuits and Systems I: Regular Papers*, vol. 60, no. 1, pp. 150–163, Jan 2013.